1521-009X/41/1/24–29$25.00
Drug Metabolism and Disposition
http://dx.doi.org/10.1124/dmd.112.048546
Drug Metab Dispos 41:24–29, January 2013

Short Communication

Evidence for Substrate-Dependent Inhibition Profiles for Human Liver Aldehyde Oxidase[S]

Received August 16, 2012; accepted September 20, 2012

ABSTRACT

The goal of this study was to provide a reasonable assessment of how probe substrate selection may impact the results of in vitro aldehyde oxidase (AO) inhibition experiments. Here, we used a previously studied set of seven known AO inhibitors to probe the inhibition profile of a pharmacologically relevant substrate *N*-[(2-dimethylamino)ethyl]acridine-4-carboxamide (DACA). DACA oxidation in human liver cytosol was characterized with a measured V_{max} of 2.3 ± 0.08 nmol product · min^{-1} · mg^{-1} and a K_m of 6.3 ± 0.8 μM. The K_{ii} and K_{is} values describing the inhibition of DACA oxidation by the panel of seven inhibitors were tabulated and compared with previous findings with phthalazine as the substrate. In every case, the inhibition profile shifted to a much less uncompetitive mode of inhibition for DACA relative to phthalazine. With the exception of one inhibitor, raloxifene, this change in inhibition profile seems to be a result of a decrease in the uncompetitive mode of inhibition (an affected K_{ii} value), whereas the competitive mode (K_{is}) seems to be relatively consistent between substrates. Raloxifene was found to inhibit competitively when using DACA as a probe, and a previous report showed that raloxifene inhibited uncompetitively with other substrates. The relevance of these data to the mechanistic understanding of aldehyde oxidase inhibition and potential implications on drug-drug interactions is discussed. Overall, it appears that the choice in substrate may be critical when conducting mechanistic inhibition or in vitro drug-drug interactions prediction studies with AO

Introduction

Aldehyde oxidase (AO) is a member of the molybdo-flavin family of enzymes, a group that is characterized by containing molybopterin and FAD groups that are essential for catalytic activity. Perhaps the most widely studied molybdo-flavin enzyme, xanthine oxidase (XO), is quite similar in structure and sequence to AO; however, the two enzymes have a marked difference in substrate affinity and specificity (Kitamura et al., 2006; Torres et al., 2007). AO has broad substrate specificity, with the ability to perform redox chemistry on a variety of functional groups (e.g., azaheterocycles, aldehydes, and iminium ions) over a wide range of substrate sizes (Pryde et al., 2010; Garattini and Terao, 2012). As a consequence, AO has a significant role in the metabolism of many different xenobiotic compounds.

In recent years, AO has garnered more interest from researchers in the field of drug metabolism. This is primarily due to the azaheterocycle-oxidase activity that the enzyme exhibits. More and more, azaheterocycle groups are found in new drugs, and the number of azaheterocycle-containing drugs has been predicted to increase (Pryde et al., 2010). Azaheterocyle moieties are typically introduced into lead compounds for a variety of reasons, including increased solubility, lower lipophilicity, and optimization of binding with the drug target. In general, these groups also lead to an increased stability of a compound to cytochrome P450 oxidation. This strategy to reduce the clearance of a drug by cytochrome P450 is often effective but ultimately leads to alternate metabolic pathways such as those mediated by AO.

This work was supported by the National Institutes of Health National Institute of General Medical Sciences (Grant GM100874).
dx.doi.org/10.1124/dmd.112.048546.
[S]This article has supplemental material available at dmd.aspetjournals.org.

A number of recent studies have increased our understanding of the role of AO in drug metabolism. However, relative to other drug clearing enzymes, such as the cytochromes P450, much is left to be explored. For example, there seems to be a large gap in the fundamental knowledge of AO inhibition and how this may relate to drug-drug interactions (DDIs).

Previous investigation revealed a predominantly mixed mode inhibition profile for human liver AO across a small panel of chemically diverse inhibitors with use of phthalazine as a probe substrate (Obach, 2004; Barr and Jones, 2011). In the present study, an overlapping set of inhibitors was screened across a larger, more pharmacologically relevant probe substrate, *N*-[(2-dimethylamino)ethyl]acridine-4-carboxamide (DACA), to assess any possible variation in inhibition mode or potency. The goal of this study was to provide a reasonable assessment of how probe substrate selection may impact the results of in vitro inhibition experiments.

Materials and Methods

Chemicals Used and Enzyme Source. Reagent grade aluminum foil, mercuric chloride, 9-oxoacridan-4-carboxylic acid, $FeCl_3$, 2-methyl-4(3*H*)-quinazolinone, estradiol, ethinyl estradiol, chlorpromazine, clozapine, menadione, domperidone, allopurinol, and hydralazine were purchased from Sigma-Aldrich (St. Louis, MO). Formic acid, HCl, KOAc, AcOH, and solvents were purchased from Thermo Fisher Scientific (Pittsburgh, PA). DACA acridone was kindly provided by Dr. William A. Denny from University of Auckland (Auckland, New Zealand). Human liver cytosol (HLC), pooled from 10 individual mixed-sex donors, was purchased from BD Biosciences (Woburn, MA).

Synthesis of DACA. The synthesis of DACA was performed in accordance with literature methods with some modifications (Atwell et al., 1987). Strips (~200 mg each) of reagent-grade aluminum foil (1.5 g, 0.055 mol) were amalgamated by immersing them for ~1 minute in a solution of mercuric chloride (6 g, 0.022 mol) dissolved in ethanol (50 ml). The strips of

ABBREVIATIONS: AO, aldehyde oxidase; DACA, *N*-[(2-dimethylamino)ethyl]acridine-4-carboxamide; DDI, drug-drug interaction; HLC, human liver cytosol; L-B, Lineweaver-Burk; LC-MS/MS, liquid chromatography-tandem mass spectrometry; XO, xanthine oxidase.

amalgamated Al foil were washed with ethanol and added one by one to a refluxing, stirring solution containing 9-oxoacridan-4-carboxylic acid (1.8 g, 7.5 mmol) and KOH (0.48 g, 8.6 mmol) dissolved in 50% aqueous ethanol (60 ml). The reaction progress was monitored by TLC, and the reaction was complete after 2 hours. Subsequently, a solution of hot 1 M KOH (35 ml) was added, and the reaction mixture was filtered. The filtered solids were then washed with hot 50% aqueous ethanol, and the collected filtrate was strongly acidified with 12M HCl and reacted with $FeCl_3$ (450 mg, 2.7 mmol) under refluxing conditions until the solution was homogenous (30 minutes). The reaction solution was clarified by filtration, and solid KOAc was slowly added to precipitate the crude product, which was immediately collected by filtration and washed with cold water. To remove impurities, the collected solid was dissolved in 1 M hot aqueous KOH, filtered, and diluted while hot with EtOH. The partially purified product was precipitated by slowly adding AcOH and immediately filtered from the solution. A yellow solid was isolated (910 mg) and characterized by MS and NMR to be acridine-4-carboxylic acid.

A suspension of crude acridine-4-carboxylic acid (900 mg, 4.0 mmol) and pure benzotriazole-1-yl-oxy-tris-(dimethylamino)-phosphonium hexafluorophosphate (5.172 g, 12 mmol) was stirred in CH_2Cl_2 (25 ml) at room temperature for 2 hours. Subsequently, the reaction mixture was cooled to 4°C, and *N*, *N*-dimethylethylenediamine (4.29 ml, 3.9 mmol) was added dropwise. The solution was brought back up to room temperature and stirred for 3 hours, after which the solvent was evaporated under reduced pressure. The crude product mixture was purified using silica gel flash chromatography (CH_2Cl_2/MeOH/NH_4OH-25%, 15:1:0.1), and crystals were formed in some fractions of the eluate. The crystals were filtered out and characterized as DACA hexafluorophosphate salt (DACAXPF$_6$; 319 mg, 0.73 mmol) with use of MS and NMR. ^{1}H NMR (300 MHz, [D6]-dimethyl sulfoxide): δ = 11.68 (t, J = 6.0 1H), 9.37 (s, 1H), 8.75 (dd, J = 7.2, 1.5, 1H), 8.44(t, J = 6.6, 2H), 8.25 (d, J = 8.1, 1H), 8.00 (t, J = 6.6, 1H), 7.75 (quint, J = 7.8, 2H), 3.94 (quart, J = 6.0, 2H), 3.43 (t, J = 6.6, 2H), 2.90 (s, 6H). ESI-MS: [M+H] = 294.

Bioassay Conditions. Incubations were performed using a modified method that was previously described (Barr and Jones, 2011). Incubation mixtures consisted of substrate (final concentration ranging from 1.6 to 100 μM for DACA) and inhibitor of varying concentration in 25 mM potassium phosphate buffer (pH, 7.4) containing 0.1 mM EDTA. Inhibitor and substrate stock solutions were made up in dimethyl sulfoxide and added to the incubation such that the total concentration of dimethyl sulfoxide was exactly 1% (v/v) for all samples.

Incubations were performed at 37°C in a shaking water bath incubator. The reaction was initiated by addition of prewarmed HLC at a final concentration of 0.05 mg of total protein/ml in the reaction mixture with a final incubation volume of 800 μl. Reaction vials were shaken in open air for 2.5 minutes and then quenched with 200 μl of 1 M formic acid, containing a known concentration of 2-methyl-4(3*H*)-quinazolinone as internal standard. To remove precipitated protein and/or insoluble contaminants, the quenched samples were centrifuged for 10 minutes at 5000 rpm with use of an Eppendorf centrifuge 5415D, and the supernatant was collected for analysis. Product formation was observed to be linear with respect to time for the reaction period of 2.5 minutes.

Liquid Chromatography-Mass Spectrometry Conditions. Samples were analyzed using an 1100 series high-performance liquid chromatography system (Agilent Technologies, Santa Clara, CA) and an API 4000 tandem mass spectrometry system manufactured by Applied Biosystems/MDS Sciex (Foster City, CA) using turbospray ESI operating in positive ion mode. Chromatography was performed on a Synergi Polar reverse-phase column (30 × 3.0 mm, 4 μm; Phenomenex, Torrance, CA).

Mobile phase A consisted of 0.05% formic acid and 0.2% acetic acid in water, and mobile phase B comprised 90% acetonitrile, 9.9% water, and 0.1% formic acid.

DACA Metabolite Quantification. With use of a flow rate of 800 μl/min, the column was equilibrated at initial conditions of 95% mobile phase A for 0.3 minutes. Chromatographic separation was performed using a linear gradient over the next 2.2 minutes to 25% mobile phase A. Mobile phase A was then held constant at 25% over 0.5 minutes, followed by a linear gradient back to 95% A over 0.5 minutes. Finally, the column was re-equilibrated to the initial conditions over the last 1 minute. The total chromatographic assay time was 4.5 minutes per sample, and the retention times for internal standard and metabolite were 1.4 and 1.8 minutes, respectively (Supplemental Fig. 1).

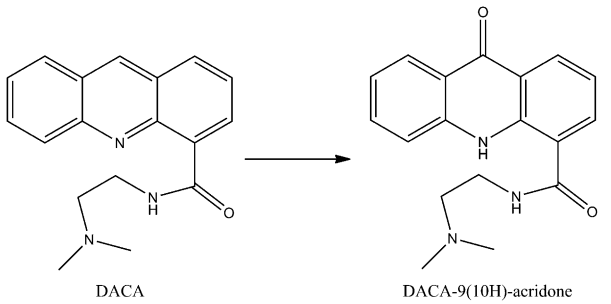

DACA DACA-9(10H)-acridone

Scheme 1. DACA oxidation reaction catalyzed by AO in HLC.

The optimized mass spectrometer tune parameters for DACA acridone were as follows: collision gas, 7; curtain gas, 15; ion source gas 1, 15; ion source gas 2, 5; ion spray voltage, 2300; desolvation temperature, 350; declustering potential, 70; entrance potential, 10; collision energy, 25; collision cell exit potential, 15.

The analyte (DACA acridone) and the internal standard [2-methyl-4(3*H*)-quinazolinone] were detected using multiple reaction monitoring mode by monitoring the *m*/*z* transition from 310 to 265 and 161 to 120, respectively. Quantitation of product was achieved by extrapolating from a standard curve ranging from a 2 to 1000 nM concentration of authentic DACA metabolite.

Data Replication and Analysis. For the first K_i assay, a minimum of six inhibitor concentrations and five substrate concentrations were used. For duplicate assays, at least four concentrations of inhibitor and four concentrations of substrate were used. Each sample was analyzed using liquid chromatography-tandem mass spectrometry (LC-MS/MS) in triplicate. Duplicate assays were performed in different experiments on different days. All reported K_i values reflect an average of the two runs.

The mode of inhibition was determined by slope and intercept replots from Lineweaver-Burk (L-B) plots along with a statistical analysis method described previously (Barr and Jones, 2011). All K_i values were calculated using a global fit to a nonlinear regression analysis using the appropriate kinetic model. All data fits and statistical analyses were performed using Prism 4 software (GraphPad Software, Inc., La Jolla, CA).

Results and Discussion

The substrate chosen for this study was an experimental antitumor agent DACA. DACA was selected as an ideal substrate for a variety of reasons. First, it is much larger, more drug-like molecule relative to a smaller probe, such as phthalazine. Second, the synthetic route to both the substrate and authentic metabolite standard are relatively straightforward. Having authentic metabolite in-hand allows for the development of a highly sensitive MS assay. Third, the rate of metabolite formation is very high, leading to a very robust assay that

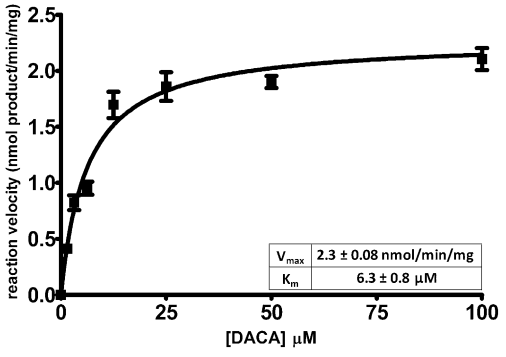

Fig. 1. Michaelis-Menten curve fit and solved kinetic parameters for the oxidation of DACA in HLC. Each point represents a mean of at least seven determinations. Solved parameters are from the best global fit ± S.E.M.

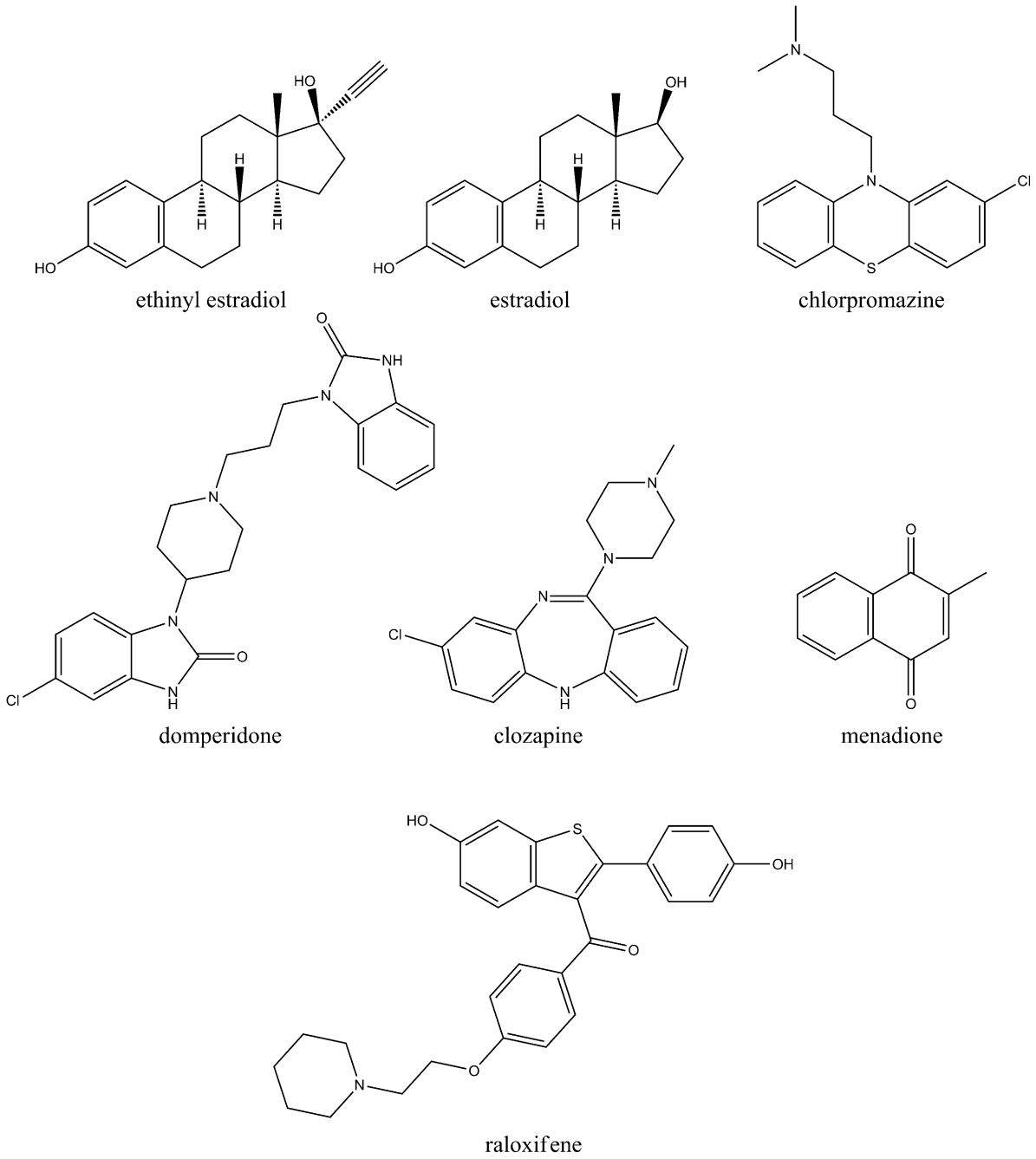

Fig. 2. Structures of AO inhibitors used in K_i studies.

works well despite short incubation times and the presence of strong inhibitors.

There is evidence for some substrate overlap between XO and AO, although AO displays much broader substrate specificity. To dispel any concerns of potential XO/AO DACA oxidase activity overlap in the cytosol, selective inhibition experiments were performed. The percentage of activities was measured for one substrate concentration around the apparent K_m for DACA and another substrate concentration in saturating conditions. Allopurinol has been characterized as a highly selective inhibitor for XO (Panoutsopoulos et al., 2004), and thus, was used to determine whether XO had a significant effect on the oxidation of DACA. In addition, to ensure that the DACA metabolism was mediated exclusively by AO, hydralazine was used as a highly specific inhibitor for AO activity (Hutzler et al., 2011; Strelevitz et al., 2012). Supplemental Fig. 2 shows the percentage of activity for DACA oxidation after addition of 100 μM of each inhibitor. After addition of allopurinol, there was no significant effect on oxidation of DACA; however, addition of hydralazine reduced activity by as much as 96%. These results indicate that DACA is highly selective for AO and there is no crossover of enzyme activity in HLC. It should be mentioned, however, that DACA is also a substrate for cytochrome P450 (Schofield et al., 1999).This was not a concern for our particular study, because there is no cytochrome P450 activity in HLC; however, it should be a consideration when working with other enzyme sources.

Saturation kinetics assays were performed with DACA using two different lots of human liver cytosol (pooled from 10 mixed-sex

donors). Scheme 1 shows the oxidation reaction of DACA by AO. The Michaelis-Menten curve fit and solved V_{max} and K_m parameters are shown in Fig. 1.

Using a DACA oxidation assay, we determined K_i values for the panel of inhibitors studied. Structures of all inhibitors are shown in Fig. 2. The K_{ii} and K_{is} values measured are listed in Table 1. K_{ii} represents the inhibition constant for the enzyme-substrate complex, and K_{is} describes the inhibition constant for the free enzyme (Cook and Cleland, 2007). K_{ii}/K_{is} was also tabulated as a coarse criterion to measure the degree of competitiveness in a given inhibition profile. A small K_{ii}/K_{is} indicates a relatively more uncompetitive mode of inhibition, whereas a large value indicates a more competitive inhibition mode.

Compared with previously measured inhibition of phthalazine, the inhibition of DACA oxidation afforded K_{ii}/K_{is} ratios that were much larger, indicating a shift toward a competitive mode of inhibition. In the case of inhibition of DACA oxidation by domperidone, clozapine, and chlorpromazine, the K_{ii}/K_{is} is not reported. The K_{ii} value for these compounds is very large or infinite because, for these three compounds, the mode of inhibition has shifted to a completely competitive mode. Figure 3 shows three examples of contrasting L-B plots and slope/intercept replots for the inhibition of phthalazine (left) and DACA (right).

A subtle yet important distinction is that the change in K_{ii}/K_{is} value is not from the inhibition becoming more competitive, but from the mode becoming less uncompetitive. This can be seen by looking at K_{is} and K_{ii} independently. In every case, with the exception of raloxifene, the K_{is} value remains relatively consistent between different substrates; however, the K_{ii} value increases 10- to 30-fold for DACA relative to phthalazine. In three cases, a K_{ii} value was not observed.

Substrate-dependent inhibition profiles in drug-metabolizing enzymes are a known phenomenon. This behavior has been observed in cytochrome P450 isoforms 3A4 (Foti et al., 2010) and 2C19 (Foti and Wahlstrom, 2008). A key difference in these cited cases is that the substrate selection seems to affect only the potency of inhibition not the mode of inhibition.

A substrate-dependent effect on K_{ii} gives insight into the mechanism by which inhibition may be occurring. A K_{ii} value is indicative of the affinity by which the inhibitor binds to the enzyme only after the substrate is bound, thereby forming an enzyme-substrate-inhibitor ternary complex. One possible explanation of the data is that the change in inhibition profile may be attributable to a large size difference between phthalazine and DACA. In the case of phthalazine, it may be possible for an inhibitor to bind within the active site even after substrate has bound. However, DACA may bind in such a way that it partially or completely occludes subsequent inhibitor binding. Another alternative explanation that cannot be excluded is that there is a secondary inhibitor binding site that is removed from the active site. When the substrate binds, the enzyme may undergo a conformational change affecting the inhibitory site. Phthalazine may bind in such a way that enhances the affinity to the inhibitory binding site (a lower K_{ii} relative to K_{is}), whereas DACA may have the opposite effect, thereby greatly decreasing the affinity the inhibitor has for the enzyme after the substrate is bound. More experiments to investigate the mechanism by which this may be occurring are currently ongoing in our laboratory.

In addition to mechanistic studies, substrate-dependent inhibition profiles also have a large impact on in vitro DDI predictions. This is primarily because of the confounding effect present when attempting in vitro to in vivo extrapolations. We have shown that the selection of in vitro substrate has a substantial impact on the mode of inhibition and, thus, the predicted DDI. When designing a DDI study, particular attention to the substrate should be paid. Perhaps use of a multiple-substrate screening approach would be appropriate. It should be noted that no clinical DDI ascribed to AO-mediated clearance has been reported in the literature. This is attributable to a number of reasons, not the least of which is a lack of clinical AO victim drugs, and of those few drugs, many have low to moderate fractional metabolic clearance ascribed to AO activity (i.e., there is a high degree of clearance overlap with other enzymes).

Raloxifene is by far the most potent AO inhibitor known and, thus, has been evaluated as a potential DDI precipitant drug using in vitro studies (Obach, 2004; Obach et al., 2004). Obach (2004) previously demonstrated that raloxifene is a potent uncompetitive inhibitor of the AO mediated oxidation of phthalazine, vanillin, and nicotine-$\Delta1'(5')$-iminium ion. Among the three substrates tested, the K_i values varied by less than 2-fold, and no change in inhibition mode was observed. Despite a high potency, raloxifene was not considered to be a high risk for DDI because of the uncompetitive nature of inhibition. However, we found that when DACA is used as a substrate, inhibition was completely competitive (L-B plot and slope replot shown in Fig. 4). Unlike the other inhibitors probed with DACA that showed a relatively constant K_{is} value, raloxifene had no observable K_{is} with phthalazine and shows a low nanomolars of K_{is} with DACA.

Because raloxifene was observed to be a highly potent, competitive inhibitor, predicting in vivo DDI is of some interest. A simple approximation can be made by the ratio $[I]/K_{is}$, where [I] is equal to the relevant concentration of drug in vivo. An $[I]/K_{is}$ greater than or

TABLE 1

Comparison of inhibition parameters for human cytosolic aldehyde oxidase-catalyzed oxidation of two different substrates

NO indicates a K_i value that was not observed and was excluded from the best fit model. ND indicates the value was not determined, because the mode of inhibition was not mixed.

Inhibitor	Phthalazine[a]			DACA		
	K_{is}	K_{ii}	K_{ii}/K_{is}	K_{is}	K_{ii}	K_{ii}/K_{is}
	μM			μM		
β-Estradiol	0.9 ± 0	0.13 ± 0	0.14	0.87 ± 0.5	4.4 ± 0.4	5.1
Menadione	0.75 ± 0.2	0.12 ± 0	0.16	0.47 ± 0.0	1.5 ± 0.5	3.2
Ethinyl estradiol	1.1 ± 0.3	0.23 ± 0.01	0.21	0.43 ± 0.2	3.6 ± 0.4	8.5
Domperidone	5.3 ± 3	14 ± 3	2.1	1.2 ± 0.2	NO	ND
Chlorpromazine	0.62 ± 0.2	3.3 ± 0.5	5.3	0.62 ± 0.07	NO	ND
Clozapine	3.9 ± 0.4	60 ± 2	15	5.1 ± 0.9	NO	ND
Raloxifene	NO	0.00087 ± 0.00005[b]	ND	0.0023 ± 0.0006	NO	ND

[a] All values for phthalazine oxidase inhibition with exception of raloxifene were previously reported in Barr and Jones (2011).
[b] Data reported from Obach (2004).

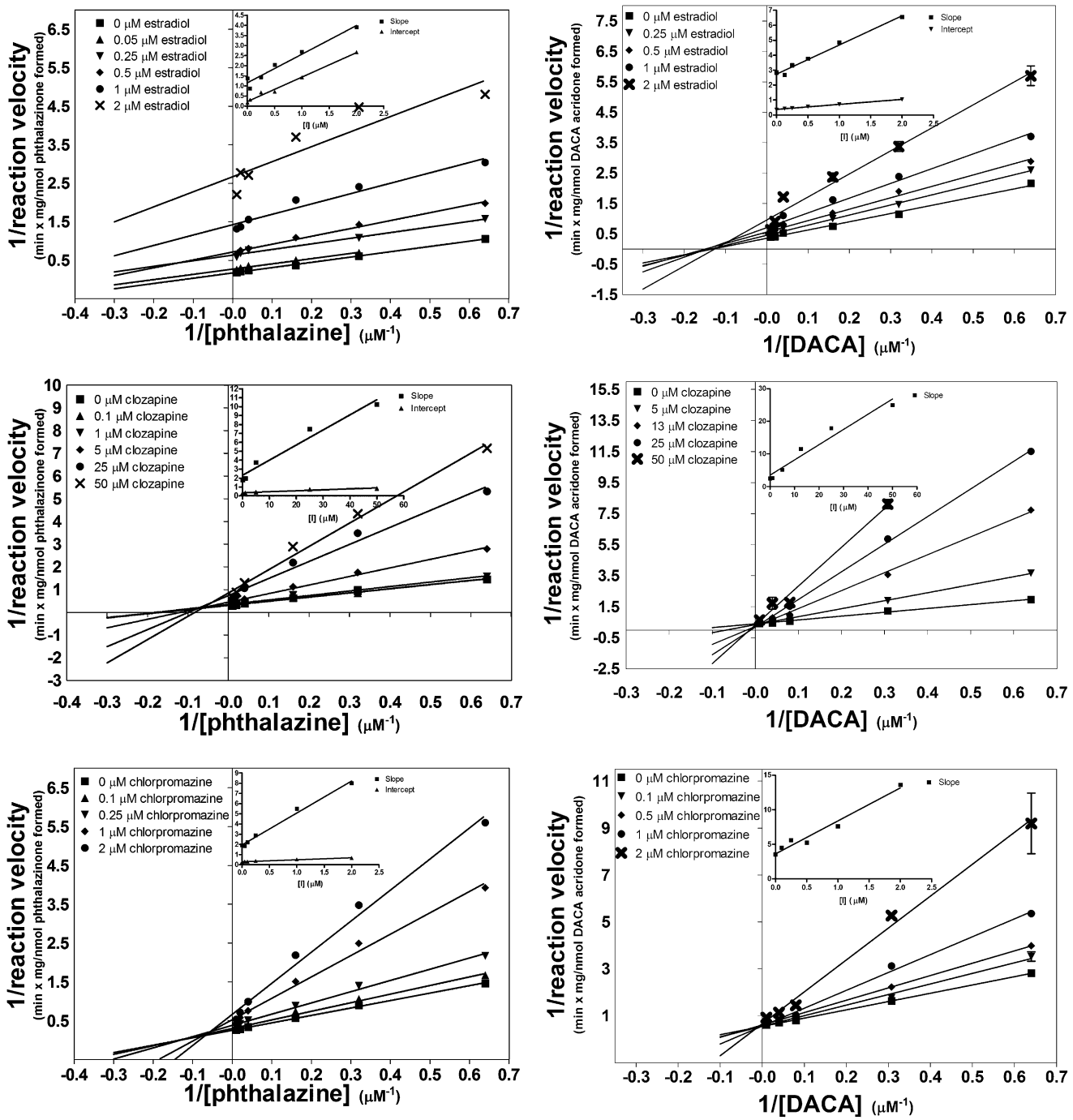

Fig. 3. L-B plots comparing the inhibition of the AO-catalyzed oxidation of two different substrates in HLC: phthalazine (left) and DACA (right). Inset graphs are subsequent replots of slope and/or *y*-intercept of the L-B plots. The top two panels show inhibition by estradiol, center panels show inhibition by clozapine, and bottom panels show inhibition by chlorpromazine. Each point represents the mean ± S.E.M. of a single assay vial analyzed in triplicate by LC-MS/MS.

equal to 1 is indicative of a high risk of DDI, 0.1–1 indicates moderate risk, and any value less than 0.1 indicates low risk (Tucker et al., 2001). Literature sources indicate an in vivo C_{max} of 2.9 nM for raloxifene following a typical chronic dosing regimen (Hochner-Celnikier, 1999). With use of this as a conservative estimate for [I], [I]/K_{is} is 1.3, meaning that raloxifene falls within the high risk range when probed with DACA, whereas it has no risk when probed with phthalazine. This clearly demonstrates that the potential for a DDI with AO will be affected by the substrate. Of note, however, the use of C_{max} for [I] tends to overpredict DDI in most cases. More sophisticated models consider the unbound concentration of the drug for estimation of [I] along with other parameters (Obach et al., 2006). Because raloxifene is 95% bound in the plasma (Hochner-Celnikier, 1999), using unbound C_{max} for [I] would predict no DDI.

In conclusion, for the panel of seven inhibitors tested, we found that the inhibition profile is affected by the selection of the substrate used to probe the kinetics. With the exception of raloxifene, this change in inhibition profile seems to be a result of a decrease in the uncompetitive mode of inhibition (an affected K_{ii} value), whereas the competitive mode (K_{is}) appears to be relatively consistent between

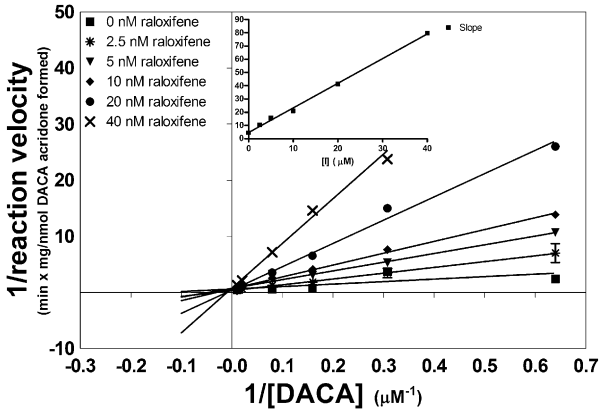

Fig. 4. L-B plot of the inhibition of AO-catalyzed DACA oxidation by raloxifene. Inset graph is a subsequent replot of L-B slopes versus inhibitor concentration. Each point represents the mean ± S.E.M. of a single assay vial analyzed in triplicate by LC-MS/MS.

substrates. We also found that raloxifene inhibits competitively when using DACA as a probe, despite a previous report that showed that raloxifene inhibited uncompetitively with other substrates. When raloxifene was treated as a competitive inhibitor and conservative estimates for [I] were used, it fell into a high-risk category as a precipitant drug for DDI. Overall, it appears that the choice in substrate may be critical when conducting mechanistic inhibition or in vitro DDI prediction studies with AO.

Acknowledgments

We thank William Denny from the University of Auckland, for kindly providing our laboratory with authentic DACA metabolite, and Upendra Dahal, for valuable discussions.

Department of Chemistry, Washington State University, Pullman, Washington

JOHN T. BARR
JEFFREY P. JONES

Authorship Contributions

Participated in research design: Barr, Jones.
Conducted experiments: Barr.
Contributed new reagents or analytic tools: Barr.
Performed data analysis: Barr.
Wrote or contributed to the writing of the manuscript: Barr, Jones.

References

Atwell GJ, Rewcastle GW, Baguley BC, and Denny WA (1987) Potential antitumor agents. 50. In vivo solid-tumor activity of derivatives of N-[2-(dimethylamino)ethyl]acridine-4-carboxamide. *J Med Chem* **30**:664–669.

Barr JT and Jones JP (2011) Inhibition of human liver aldehyde oxidase: implications for potential drug-drug interactions. *Drug Metab Dispos* **39**:2381–2386.

Cook PB and Cleland WW (2007) *Enzyme Kinetics and Mechanism*, Garland Science, New York.

Foti RS, Rock DA, Wienkers LC, and Wahlstrom JL (2010) Selection of alternative CYP3A4 probe substrates for clinical drug interaction studies using in vitro data and in vivo simulation. *Drug Metab Dispos* **38**:981–987.

Foti RS and Wahlstrom JL (2008) CYP2C19 inhibition: the impact of substrate probe selection on in vitro inhibition profiles. *Drug Metab Dispos* **36**:523–528.

Garattini E and Terao M (2012) The role of aldehyde oxidase in drug metabolism. *Expert Opin Drug Metab Toxicol* **8**:487–503.

Hochner-Celnikier D (1999) Pharmacokinetics of raloxifene and its clinical application. *Eur J Obstet Gynecol Reprod Biol* **85**:23–29.

Hutzler JM, Yang YS, Albaugh D, Fullenwider CL, Schmenk J, and Fisher MB (2012) Characterization of aldehyde oxidase enzyme activity in cryopreserved human hepatocytes. *Drug Metab Dispos* **40**:267–275.

Kitamura S, Sugihara K, and Ohta S (2006) Drug-metabolizing ability of molybdenum hydroxylases. *Drug Metab Pharmacokinet* **21**:83–98.

Obach RS (2004) Potent inhibition of human liver aldehyde oxidase by raloxifene. *Drug Metab Dispos* **32**:89–97.

Obach RS, Huynh P, Allen MC, and Beedham C (2004) Human liver aldehyde oxidase: inhibition by 239 drugs. *J Clin Pharmacol* **44**:7–19.

Obach RS, Walsky RL, Venkatakrishnan K, Gaman EA, Houston JB, and Tremaine LM (2006) The utility of in vitro cytochrome P450 inhibition data in the prediction of drug-drug interactions. *J Pharmacol Exp Ther* **316**:336–348.

Panoutsopoulos GI, Kouretas D, and Beedham C (2004) Contribution of aldehyde oxidase, xanthine oxidase, and aldehyde dehydrogenase on the oxidation of aromatic aldehydes. *Chem Res Toxicol* **17**:1368–1376.

Pryde DC, Dalvie D, Hu Q, Jones P, Obach RS, and Tran T-D (2010) Aldehyde oxidase: an enzyme of emerging importance in drug discovery. *J Med Chem* **53**:8441–8460.

Schofield PC, Robertson IG, Paxton JW, McCrystal MR, Evans BD, Kestell P, and Baguley BC (1999) Metabolism of N-[2-(dimethylamino)ethyl]acridine-4-carboxamide in cancer patients undergoing a phase I clinical trial. *Cancer Chemother Pharmacol* **44**:51–58.

Strelevitz TJ, Orozco CC, and Obach RS (2012) Hydralazine as a selective probe inactivator of aldehyde oxidase in human hepatocytes: estimation of the contribution of aldehyde oxidase to metabolic clearance. *Drug Metab Dispos* **40**:1441–1448.

Torres RA, Korzekwa KR, McMasters DR, Fandozzi CM, and Jones JP (2007) Use of density functional calculations to predict the regioselectivity of drugs and molecules metabolized by aldehyde oxidase. *J Med Chem* **50**:4642–4647.

Tucker GT, Houston JB, and Huang S-M (2001) Optimizing drug development: strategies to assess drug metabolism/transporter interaction potential—toward a consensus. *Pharm Res* **18**: 1071–1080.

Address correspondence to: Jeffrey P. Jones, Washington State University, Fulmer Synthesis Building, Room 477, Pullman, WA 99164-4630. E-mail: jpj@wsu.edu